ELSEVIER

Polymer 42 (2001) 6199–6207

polymer

www.elsevier.nl/locate/polymer

Tensile and elastic properties of segmented copolyetheresteramides with uniform aramid units

M.C.E.J. Niesten[1], R.J. Gaymans*

Laboratory of Polymer Technology, Department of Chemical Technology, University of Twente, P.O. Box 217, 7500 AE Enschede, The Netherlands

Received 21 February 2000; received in revised form 26 January 2001; accepted 26 January 2001

Abstract

The tensile and elastic properties of segmented copolyetheresteramides with crystallisable aramid units of uniform length were investigated. The aramid concentration ranged from 3 to 30 wt%. The effect of type of poly(tetramethyleneoxide) (PTMO) segment, having a different tendency to crystallise, on the tensile and elastic properties was studied. The fracture stress of the polymers was found to be mainly affected by the degree of strain-induced crystallisation of the PTMO phase and the molecular weight of the polymers and not by the aramid content. The fracture strain of the polymers is exceptionally high, ranging from 1300 to 2200%. The shear modulus increased strongly with aramid content and ranged from 1.5 to 118 MPa. The uniform aramid units are very effective in forming physical crosslinks. The yield stress increased linearly with the aramid content. The yield stress and the log modulus are nearly linearly related for materials with these uniform length crystallisable units. The change of the modulus as a function of prestrain was studied. Up to 160–180% pre-strain the modulus decreases by a factor of 6–8, however, at higher strains the moduli increased again. The strong strain softening effect in the first 160% strain must be due the breaking up of the interconnecting lamellar structure. The healing of the modulus of strain-softened samples was studied with time. The healing was very slow. The materials, especially the low-modulus types, are highly elastic. The stress relaxation decreases with decreasing aramid content and the compression set was found to have a minimum at 9 wt% aramid. As expected, (strain-induced) PTMO crystallisation influences the elasticity and low-temperature flexibility negatively.

Keywords: Copolyetheresteramides; Tensile properties; Elastic properties

1. Introduction

Segmented copolymers such as copolyetheresters or segmented polyurethanes possesses a high tensile strain comparable to chemically crosslinked rubbers ranging from 500 to 800%, while their tensile stress is higher than that of chemically crosslinked rubbers, i.e. 20–50 MPa for copolyetheresters and polyurethanes and 10–30 MPa for chemically crosslinked rubbers [1]. However, the elastic recovery after applied deformation is usually lower than that of chemically crosslinked rubbers.

Segmented copolyetheresteramides with uniform amide units like TΦT–PTMO segmented copolymers (Fig. 1) are an interesting type of thermoplastic elastomers. The TΦT segments crystallise very fast and the copolymer possess a low T_g (−65°C) and sharp melting temperature [2,3]. The shear modulus is little temperature-dependent and ranges from 1.5 to 118 MPa with increasing TΦT content. The strong effect of the TΦT content on the modulus has been explained as being due to the complete crystallisation of these units.

In homopolymers, the crystalline phase formed from the melt consists of lamellae, which are stacked into spherulites. The lamellae in the spherulite have an interconnecting structure [4–6]. Segmented copolymers, which are crystallised from a homogeneous melt, can form spherulitic structures too [7] and at fast cooling (high nucleation rates) intermeshing bundles of lamellae having a high aspect ratio without a sharp spherulitic boundary are formed [7,8]. The lamellae have often a ribbon-like structure. From this, it can be expected that the TΦT units in our polymers, which crystallise from a homogeneous melt form lamellae with a high aspect ratio, which are interconnected. A schematic structure of stacked lamellae having a high aspect ratio and which are interconnected is given in Fig. 2. The crystalline lamellae (C) act as physical crosslinks for the amorphous phase (A). Additionally, a crystalline PTMO phase is present if PTMO segments longer than 1000 g/mol are used.

The presence of a yield point in the stress–strain curve of segmented copolymers also indicates the existence of an

* Corresponding author.
E-mail address: r.j.gaymans@ct.utwente.nl (R.J. Gaymans).
[1] Presently at Huntsman Polyurethanes, Everberg, Belgium.

0032-3861/01/$ - see front matter
PII: S0032-3861(01)00088-X

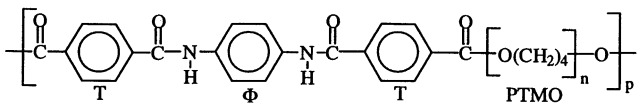

Fig. 1. Structure of segmented copolymer TΦT–PTMO.

interconnecting crystalline hard phase [1,9]. For polyethylene, the yield stress increases with crystallinity and lamellar thickness [10,11]. The effect of only the crystallinity on the yield stress can be studied on segmented polymers with crystalline lamellae of uniform thickness. The modulus is highly dependent on the structure of the crystalline phase and hence also on the crystallinity. The increase of the modulus (E) with crystallinity (v_c) has been described by Eq. (1) [9]:

$$\log E = v_c \log \frac{E_c}{E_a} + \log E_a \quad (1)$$

where E_c is the modulus of the crystalline fraction and E_a the modulus of the amorphous fraction.

Upon straining a segmented polymer, the soft segments are stretched thereby exercising forces on the crystalline hard domains. Up to about 200% strain, the soft segments start to orient and the interconnecting lamellar structure is disrupted [8,13,14]. At the same time, the lamellae are oriented with their long axis in the strain direction. At higher strains, the crystalline lamellae are fully broken up into small units and these units are now oriented with the polymer chain in the deformation direction. The breaking up process of the interconnecting crystalline structure leads to strain softening of the materials [9]. In styrene–butadiene–styrene (SBS) block copolymers, the strain-softening phenomenon has been attributed to a morphology change from alternating lamellar domains to fragmented polystyrene domains dispersed in the polybutadiene matrix [15]. After storage of the sample in the unstrained state for several days at room temperature, the fragmented polystyrene domains are transformed into the original lamellar domains, a healing process. The question is whether with semi-crystalline segments healing can also take place. Using AFM microscopy, a healing process has also been described for poly(etheramide) segmented copolymers [16].

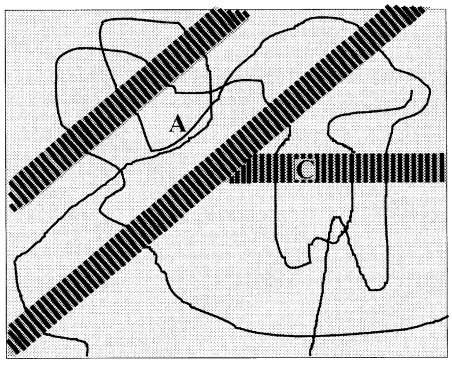

Fig. 2. Schematic representation of morphology of crystallised segmented copolymers: C, crystalline lamellae; A, amorphous PTMO phase.

The soft segment type also plays an important role in the mechanical and elastic properties of segmented copolymers. Soft segments, which strain crystallise produce materials with a higher tensile strength, but also a higher tensile set. An upturn in the tensile curve at high strains is often taken as evidence of strain-induced crystallisation (strain hardening) [1].

The deformation behaviour of copolymers with uniform crystallisable segments has been studied little. Harrell [17] observed that segmented polyurethanes with a narrow hard segment length distribution have improved mechanical properties (higher modulus, higher tensile strain and stress) compared to similar polymers with broad hard segment length distributions. The tensile set, however, was also higher, which was explained by the improved phase separation and consequently higher crystallinity. Van Hutten et al. [18] studied segmented copolyetheresteramides with the uniform 1,4-butylene terephthalamide (T4T) crystallisable units and poly(tetramethyleneoxide) (PTMO) soft segments. With decreasing T4T content, the stress–strain curves obtained an elastomeric character, showing a low initial modulus, a sigmodial curve and a fracture strain exceeding 1000%.

In this study, the effect of the hard segment concentration and type of poly(tetramethyleneoxide) (PTMO) on the tensile and elastic properties of segmented copolymers with uniform aramid hard segments (TΦT) and PTMO-based soft segments is studied. Several tensile properties, such as the yield stress, ultimate tensile properties, strain hardening, strain softening and healing of the structure with time are evaluated. As a measure of the elasticity of the materials, stress relaxation and compression set experiments are carried out.

2. Experimental

2.1. Polymerisation

The polymerisation and soft segment length calculation are described in previous publications [2,3].

2.2. Viscometry

The inherent viscosity of the polymers at a concentration of 0.1 g/dl in a 1/1 (molar ratio) mixture of phenol–1,1,2,2-tetrachloroethane at 25°C, was determined using a capillary Ubbelohde 1B.

2.3. Sample preparation

Samples for the tensile tests were prepared by melt extruding the polymers into threads on a 4 cc DSM Res RD11H corotating twin screw mini extruder. The extruder temperature was set at 60°C above the flow temperature of

the polymers, while the screw speed was kept constant at 30 rpm. The threads (about 100 μm diameter) were winded at a speed range from 20 to 50 m/min. To calculate the stress, the linear density of the threads was determined. The linear density (expressed in tex $= 10^{-6}$ kg/m) of the threads was measured by carefully weighing 1 m of thread. The density of the polymers was determined in hexane and was approximately 1.0 g/cm^3.

Samples for DMA test, stress relaxation experiments and compression set test ($70 \times 9 \times 2$ mm^3) were prepared on a small-scale plunger injection molding machine, type Arburg H. The barrel temperature of the injection-molding machine was set at 50°C above the melting temperature of the polymer, while the mould temperature was kept at room temperature.

2.4. Dynamic mechanical analysis

Using a Myrenne ATM3 torsion pendulum at a frequency of approximately 1 Hz, the values of the shear modulus G' as a function of the temperature were measured. Dried samples were first cooled to −100°C and then subsequently heated at a rate of 1°C/min with the maximum of the loss modulus being taken as the glass transition temperature.

2.5. Tensile tests

Tensile tests were carried out on a Zwick Z020 universal tensile machine equipped with a 10 N load cell, the strain being measured as the clamp displacement. Stress–strain curves were obtained at a strain rate of 250 mm/min, the starting clamp distance being 25 mm.

2.6. Cyclic tensile tests

Cyclic tensile tests were carried out on a Zwick Z020 universal tensile machine equipped with a 10-N load cell, the strain being measured as the clamp displacement. Cyclic stress–strain curves were obtained at a straining rate of 200 mm/min, the starting clamp displacement being 50 mm. Until 100% strain, the strain increased 20% each cycle, followed by a strain increase of 100% each cycle until the sample broke. The modulus at the start of each load cycle was determined manually at approximately 5% strain and corrected for the changed sample dimensions. Healing of the initial modulus was measured after applying a 300% cyclic strain. Before starting the second cycle, a healing time was introduced varying from 0 to 64 h.

2.7. Stress relaxation

Injection-moulded test bars were used as samples for the stress relaxation experiments. The stress relaxation was measured on a Zwick Z020 universal tensile machine equipped with a 500 N load cell, the strain being measured as the clamp displacement with a starting clamp distance of 40 mm. The samples were strained to 25% or 100% within 5 s at room temperature. The decay of the stress was measured during 30 min. As a measure of the stress relaxation ($SR_{x\%}$), the absolute value of the slope of the line, obtained from the stress plotted versus the logarithm of time, was used (Eq. (2)).

$$SR_{x\%} = \frac{|\Delta\sigma_{x\%}|}{\Delta \log t} \quad [-] \tag{2}$$

2.8. Compression set

A piece of an injection-moulded test bar, similar to those used for stress relaxation was placed between two steel plates and compressed to 1 mm (≈55% compression). After 24 h at room temperature or at 70°C, the compression was released at room temperature. One hour later, the thickness of the sample was measured. The compression set (Eq. (3)) was defined as:

$$\text{Compression set} = \frac{d_0 - d_2}{d_0 - d_1} \times 100\% \tag{3}$$

where d_0 is the thickness before compression (mm), d_1 the thickness during compression (mm) and d_2 the thickness 1 h after release of compression (mm).

3. Results and discussion

The tensile and elastic properties of polymers with varying TΦT concentration and different PTMO-based soft segments are studied. The following types of PTMO are compared (Fig. 3): PTMO, modified PTMO (PTMOm, containing 15 wt% of methyl side groups) and extended PTMO with dimethyl terephthalate or dimethyl isophthalate (PTMO/DMT or PTMO/DMI). Firstly, the relationship between the modulus and the crystallinity is described. Then several tensile properties are discussed, followed by strain softening, expressed as the decrease of the initial modulus after a cyclic tensile test. The healing of the initial modulus of the second load cycle is discussed. Finally, the results of stress relaxation and compression set experiments are given.

In Table 1, an overview of the mechanical properties of the polymers is given. The TΦT contents given were calculated on the basis that the ester group attached to the amide units did not belong to TΦT unit. The ester groups were found to orient on straining similar to the ether units and different than the amide units [13]. The TΦT concentration of the polymers ranged from 3 to 31 wt%. All the polymers have a high inherent viscosity indicating that they have all a high molecular weight.

3.1. Relationship between modulus and crystallinity

In Fig. 4, the logarithm of the shear modulus at 25°C is plotted versus the TΦT content. The modulus increases strongly with concentration. The TΦT units are thus very efficient in increasing the modulus. As the TΦT did not

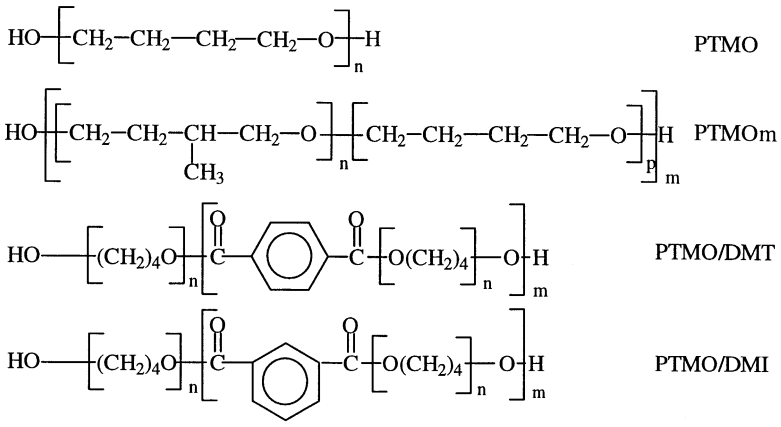

Fig. 3. Structure of types of PTMO used.

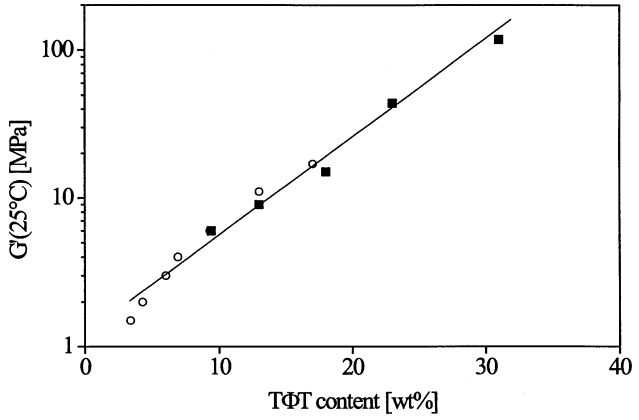

Fig. 4. Logarithm of the shear modulus versus TΦT content: (■), TΦT–PTMO; (○), TΦT–(PTMO$_{1000}$/DMT).

influence the T_g of the PTMO phase and a separate glass transition was not found, it was concluded that most of the TΦT have crystallised [2,3]. According to Wegner [9], the logarithm of the modulus in the rubbery region of a segmented copolymer follows a linear relationship with the crystallinity (Eq. (1)). The TΦT–PTMO polymers follow this relationship too. It is concluded that Eq. (1) is useful for describing the increase of the modulus with crystallinity.

3.2. Stress–strain behaviour

Stress–strain curves were determined using extruded threads. The TΦT concentration and the type of PTMO segment strongly affect the tensile behaviour (Table 1). In Fig. 5, some stress–strain curves of TΦT–PTMO (a) and TΦT–(PTMO-based)$_{2000}$ (b) copolymers are shown. The different characteristics of the tensile curves will be discussed in the following.

3.2.1. Fracture strain

The fracture strain is surprisingly high, ranging from 1300 to 2060% ($\lambda = 14$–21.6). The softer materials in the series do not have a higher fracture strain and thus the fracture strain does not seem to be related to the PTMO

Table 1
Properties of TΦT–PTMO polymers. (η_{inh}, inherent viscosity; G'(25°C), shear modulus at 25°C; σ_y, yield stress, σ_b: fracture stress, λ_b, fracture strain)

Polymer	TΦT (wt%)	Soft segment (g/mol)	η_{inh} (dl/g)	G'(25°C) (MPa)	σ_y (MPa)	σ_b (MPa)	e_b (-)
TΦT–PTMO$_{650}$	31	650	1.40	118	14.0	–	–
TΦT–PTMO$_{1000}$	23	1000	1.81	44	9.8	38.1	14.7
TΦT–PTMO$_{1400}$	18	1400	1.92	15	–	–	–
TΦT–PTMO$_{2000}$	13	2000	2.20	10	5.7	51.9	17.6
TΦT–PTMO$_{2900}$	9.6	2900	2.74	6	3.4	58.8	16.6
TΦT–(PTMO$_{1000}$/DMT)$_{1500}$	17	1500	1.74	17	6.6	17.0	17.4
TΦT–(PTMO$_{1000}$/DMT)$_{2000}$	13	2000	1.48	11	5.5	9.2	18.4
TΦT–(PTMO$_{1000}$/DMT)$_{3000}$	9.3	3000	2.07	6	3.7	13.0	21.6
TΦT–(PTMO$_{1000}$/DMT)$_{4200}$	6.9	4200	2.23	4	3.1	21.3	14.8
TΦT–(PTMO$_{1000}$/DMT)$_{6000}$	4.9	6000	2.29	3	2.7	25.2	14.0
TΦT–(PTMO$_{1000}$/DMT)$_{7000}$	4.3	7000	1.31	2	–	–	–
TΦT–(PTMO$_{1000}$/DMT)$_{9000}$	3.4	9000	1.67	1.5	1.2	15.2	21.7
TΦT–(PTMO$_{1000}$/DMI)$_{2000}$	13	2000	1.70	11	5.4	19.2	19.4
TΦT–(PTMO$_{1000}$/DMI)$_{3150}$	8.9	3150	2.37	6	3.7	25.0	15.3
TΦT–(PTMO$_{650}$/DMT)$_{2000}$	13	2000	1.56	11	5.3	7.60	20.9
TΦT–PTMO$_{2000m}$	13	2000	2.04	10	5.6	27.2	17.6

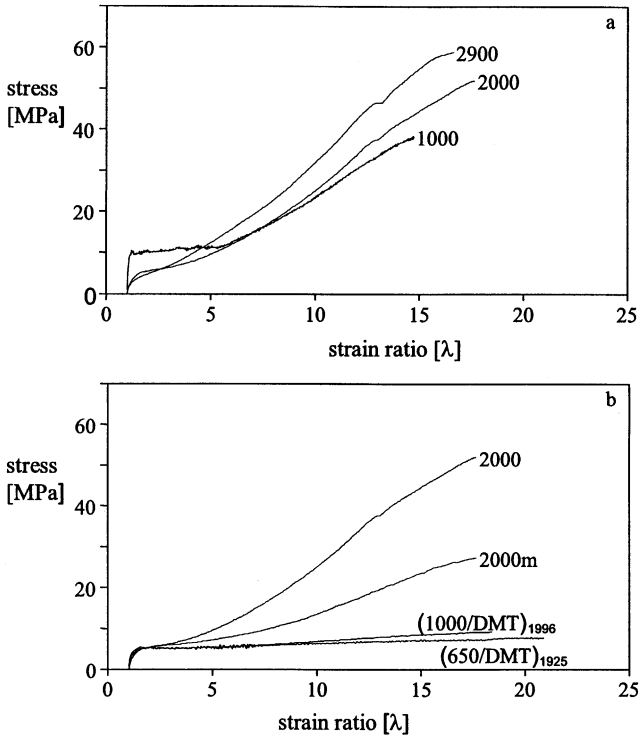

Fig. 5. Stress–strain curves of: (a) TΦT–PTMO; (b) TΦT–(PTMO-based)$_{2000}$ copolymers.

length and the TΦT concentration (Table 1). Harrell [17] and Miller [19] already observed a higher fracture strain for segmented polyurethanes with a narrow hard segment length distribution than for similar polyurethanes with a broad segment length distribution. This might be explained as follows: if a segmented copolymer is strained, first the soft segments are stretched. Since there is a distribution of soft segment lengths, the crystalline lamellae need to be deformed to stretch all the soft segments to the same extent. More force is needed to deform thick lamellae and therefore, the limiting factor in stretching a segmented copolymer with non-uniform hard segments are the thick lamellae present. In our polymers, however, there is only one size, very thin lamellae (1.8 nm, length of TΦT unit) present, which are expected to have a limited resistance to plastic deformation making stretching the soft segments to their full extent rather easy.

3.2.2. Fracture stress

The fractures stresses in these copolymers depend on the type of PTMO used and can be high (Table 1 and Fig. 5). Increasing the PTMO molecular weight lowers the yield stress but increases the fracture stress (Fig. 5a). At a strain of about 300% strain, hardening seem to take place. Longer PTMO segments are known to crystallise more easily and strain harden more strongly [20]. The fracture strains even seem to increase with increasing PTMO molecular weight, but this might be a effect due to the differences in polymer molecular weight (Table 1). The true fracture stresses of the

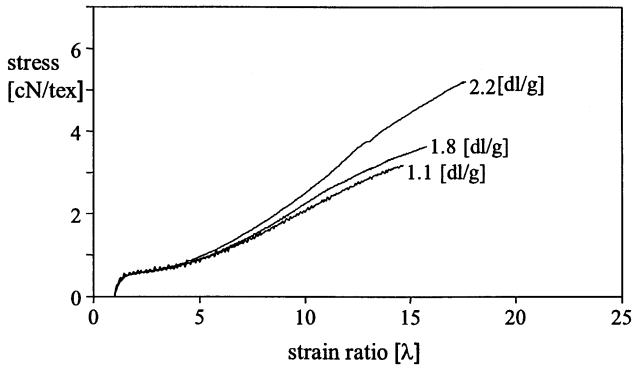

Fig. 6. Stress–strain curves of TΦT–PTMO$_{2000}$ with different inherent viscosities.

PTMO$_{2900}$ approached a value of 1 GPa, which is remarkably high for a soft material.

At a constant PTMO molecular weight (2000 g/mol), the structural regularity of the PTMO has a strong effect on strain hardening, but little on the fracture strain (Fig. 5b). The 2000 has a much higher fracture stress than the (1000/DMT)$_{2000}$ or (1000/DMI)$_{2000}$ and the 2000m has a value in-between. Thus the strain-induced crystallisation is reduced by using PTMO$_{2000m}$ or even further by incorporating DMT or DMI in the PTMO phase. Chemical irregularities restrict crystallisation of the PTMO phase [3]. The fracture stress is strongly affected by the amount of strain-induced crystallisation.

Increasing the soft segment length in PTMO/DMT polymers seem to have little effect on the fracture strain (Table 1). So here the length of the polyether has little effect on the strain hardening. These results also suggest that the TΦT content has little effect too. The fracture strain data are, however, erratic. It seems that there is an effect of the polymer molecular weight (η_{inh}) on the fracture strain.

In general, the fracture stresses of polymer increase with molecular weight [21,22]. The polymer molecular weight effect in these polymers was studied with PTMO$_{2000}$ (Fig. 6). Increasing the polymer molecular weight strongly increases the fracture stress. Going from η_{inh} 1.1 to 2.2, the true fracture stress increases from 470 to 915 MPa. Up to 600% strain, the curves coincide but at higher strains, the slopes of the curves become steeper with increasing molecular weight. This may be explained by the fact that longer chains have a higher entanglement density and as a result of this can be more oriented. Thus for optimal tensile properties, a high molecular weight polymer is important here.

3.2.3. Yield stress

The stress–strain curve of TΦT–PTMO$_{1000}$ has a distinct yield point (Fig. 5a) indicating the presence of an interconnected hard phase [1,12]. Although the threads are thin, some necking was observed for this polymer. In the other polymers, which have a lower TΦT content, necking was not visible. With increasing PTMO length and

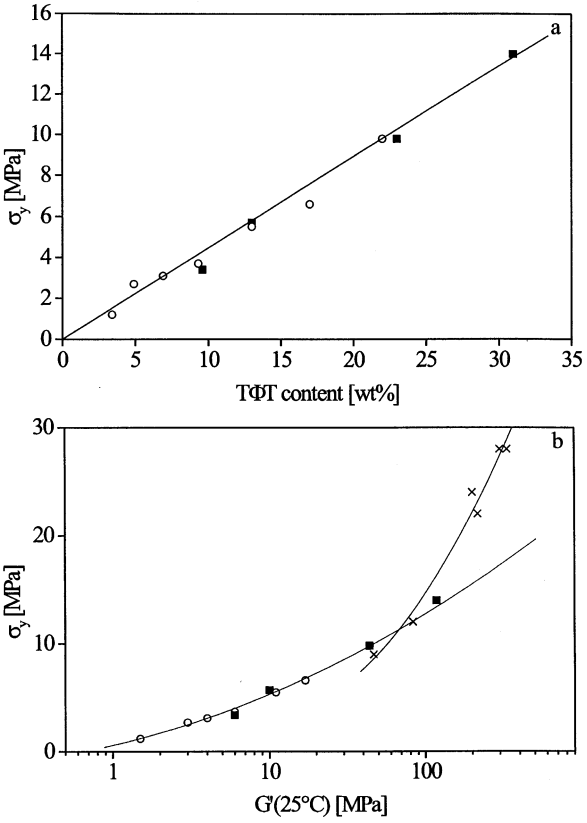

Fig. 7. Yield stress (σ_y) versus (a) TΦT content and (b) logarithm of shear modulus (G'(25°C)) for: (■), TΦT–PTMO; (○), TΦT–(PTMO$_{1000}$/DMT); (×), polyethylene (Ref. [23]).

consequently decreasing TΦT content, the yield stress decreases and becomes less pronounced. In Fig. 7a, the yield stress is plotted as function of TΦT content (a) and the logarithm of the shear modulus at 25°C (b) for the TΦT–PTMO and TΦT–(PTMO$_{1000}$/DMT) series. The yield stress increased linearly with the TΦT content. Assuming that nearly all the TΦT units are in the crystalline phase, it is clear that the yield stress increase linearly with crystallinity. This is a perfect example of polymers in which the yield stress depends solely on the crystallinity since the thickness of the crystalline lamellae with amide units of uniform length is constant.

The yield stress and the modulus are known to be related [23]. The yield stress is plotted versus the log shear modulus. A fairly linear relationship is obtained (Fig. 7b). This was expected from Figs. 4 and 7. In Fig. 7b, data of polyethylene are also included [24]. The points for the yield stress of PE lie above the extrapolated curve of the TΦT–PTMO copolymers. In polyethylene, both the crystallinity as well as the lamellar thickness is changed. The strong increase in yield stress for polyethylene might be caused by the increasing lamellar thickness of the polyethylene samples with crystallinity.

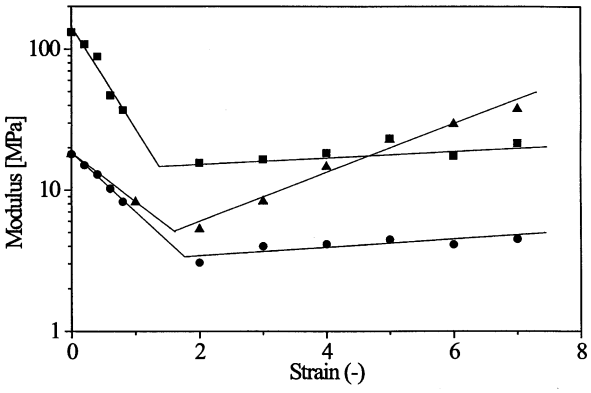

Fig. 8. Influence of pre-straining on modulus for: (■),TΦT–PTMO$_{1000}$; (▲), TΦT–PTMO$_{2900}$; (●),TΦT–(PTMO$_{1000}$/DMT)$_{3000}$.

3.3. Strain softening

Samples were strained for a certain amount and the modulus of the strained sample redetermined (Fig. 8). The modulus was found to decrease strongly in the first 160–180%. The decrease is about a factor of 6–8 for three studied samples with different PTMOs. The decrease is thus proportional to the modulus of the undeformed material. The type of PTMO and the concentration of TΦT seem to have little effect on the strain softening effect. Thus the crystallinity has little effect either. After higher strains, the modulus increases again and this increase is strong for the polymer with the easily strain hardening PTMO$_{2900}$ segment.

Strain softening is caused by disruption of the crystalline structure upon straining [10,13,16]. In the first 160–180% strain, two opposing processes take place: the interconnecting crystalline structure is broken up and the crystalline lamellae, still having a high aspect ratio, are oriented in the straining direction (Fig. 9a and b). From lamellae having a high aspect ratio and oriented in the strain direction, one would expect an appreciable reinforcing effect, however, we see a strong lowering of the modulus. This means that the breaking up of the interconnecting crystalline structure is even more important for the modulus.

After higher strains, the modulus increases again. During this process, the oriented lamellae are broken up, the small lamellar units turn around and the amorphous phase starts to orient (Fig. 8b and c). The net effect of these processes is a slight increase in modulus. Hence the orientation of the amorphous phase has thus a larger effect than the loss in aspect ratio of the lamellae. Strain hardening of PTMO$_{2900}$ increases the overall crystallinity of the polymer and this has a clear effect on the modulus (Fig. 8).

3.4. Healing

Polymers are viscoelastic materials, their response to

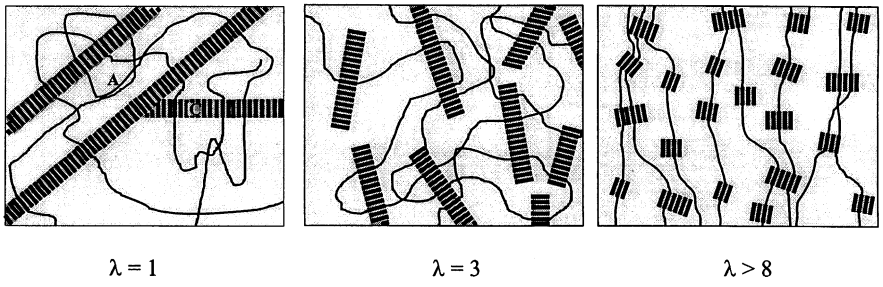

Fig. 9. Schematic presentation on the changes in structure on straining.

deformation is time-dependent, not only for the amorphous phase but also for the crystalline phase. The relaxation/healing can be studied in a cyclic test. In Fig. 10, an example of hystereses, strain softening and relaxation process between the first unloading and the second loading cycle is shown for TΦT–$PTMO_{1000}$. From this figure, it is clear that the modulus of the second load cycle increases with the relaxation/healing time. The increase of the modulus with time for some polymers after a first loading cycle of 300% is given in Fig. 11. The modulus slightly increases with the log of the relaxation/healing time. This increase seems to be little dependent on the TΦT content and the PTMO length. The relaxation of the amorphous phase is not expected to increase the modulus. The small crystallites of the disrupted crystalline network apparently have the mobility to aggregate again probably due to the flexibility of the amorphous phase. Extrapolating to the starting modulus, it would take some 10^4 years to reach the original modulus.

3.5. Stress relaxation and compression set

In an ideal elastomer, no stress relaxation occurs, as there is no plastic deformation. Generally, a lower stress relaxation value corresponds with a lower permanent deformation [25]. If, for the studied polymers studied, the stress is plotted versus the logarithm of time (σ–log t plot), a curve with two slopes is obtained indicating that two relaxation mechanisms occur. During the first 25 s, a region which is difficult to measure, the slope of the curve is 3–10 times steeper than the slope of the rest of the curve (the higher the TΦT content, the steeper the initial slope). The stress relaxation was defined as the value of the second slope at 25 or 100% strain and the results are given in Table 2 and Fig. 12a.

The stress relaxation values are plotted versus the TΦT content for TΦT–PTMO and TΦT–($PTMO_{1000}$/DMT) (Fig. 12a). As expected, the stress relaxation decreases with decreasing TΦT content. These results indicate that the plastic deformation becomes very low at low aramid contents. The stress relaxation at 100% strain of TΦT–$PTMO_{2900}$ (9.6 wt% TΦT) is higher than that of TΦT–($PTMO_{1000}$/$DMT)_{3000}$ (9.3 wt% TΦT) despite the nearly same TΦT content; this probably due to crystallisation of the $PTMO_{2900}$ segments resulting in a higher overall crystallinity.

The compression set is defined in such a way that a low residual deformation results in a low compression set value.

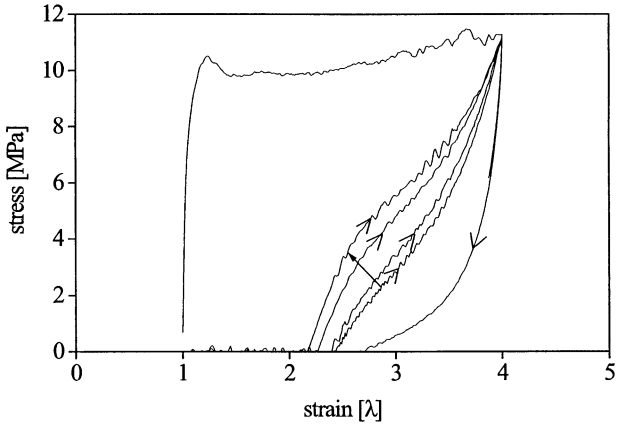

Fig. 10. Cyclic tensile test for TΦT–$PTMO_{1000}$, healing time between unloading and second loading cycle, time increases in direction of arrow: 0 s, 30 s, 30 min, 16 h.

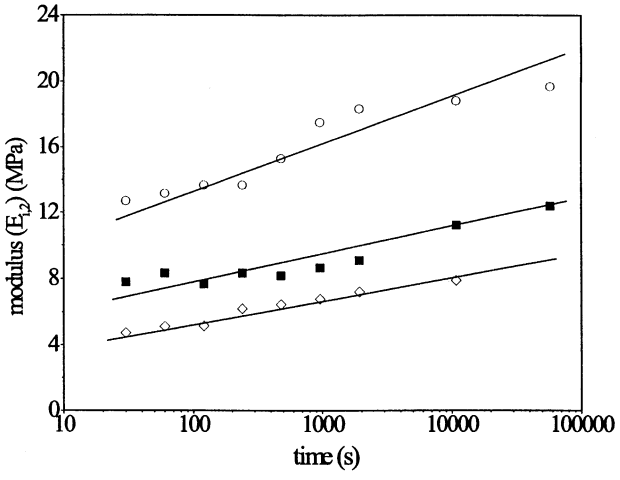

Fig. 11. Influence of healing time on modulus after a 300% pre-strain for: (○), TΦT–$PTMO_{1000}$; (■), TΦT–$PTMO_{2900}$; (◇), TΦT–($PTMO_{1000}$/$DMT)_{3000}$.

Table 2
Stress relaxation and compression set data

Polymer	$SR_{25\%}$ (%)	$SR_{100\%}$	Compression set 55%, $T = 20$°C	Compression set 55%, $T = 70$°C
TΦT–$PTMO_{1000}$	0.68	0.82	31	48
TΦT–$PTMO_{1400}$	0.37	0.70	21	48
TΦT–$PTMO_{2000}$	0.21	0.48	19	42
TΦT–$PTMO_{2900}$	0.11	0.37	22	40
TΦT–$(PTMO_{1000}/DMT)_{2000}$	0.21	0.47	17	38
TΦT–$(PTMO_{1000}/DMT)_{3000}$	0.11	0.29	13	38
TΦT–$(PTMO_{1000}/DMT)_{4000}$	0.10	0.27	15	47
TΦT–$(PTMO_{1000}/DMT)_{5000}$	0.09	0.24	24	55
TΦT–$(PTMO_{1000}/DMT)_{7000}$	–	0.15	21	66
TΦT–$(PTMO_{1000}/DMT)_{9000}$	0.06	0.14	23	67
TΦT–$(PTMO_{1000}/DMI)_{2000}$	0.23	0.48	25	52
TΦT–$(PTMO_{650}/DMT)_{2000}$	0.25	0.44	17	42
TΦT–$PTMO_{2000m}$	0.25	0.43	21	45

The compression set values are given in Table 2 and Fig. 12b. The compression set values decrease with decreasing TΦT contents up to 9 wt%, however at TΦT contents lower than 9 wt% the compression set increased again. Apparently, at very low TΦT concentrations, the physical crosslink density is too low to prevent plastic flow in this 24- h test.

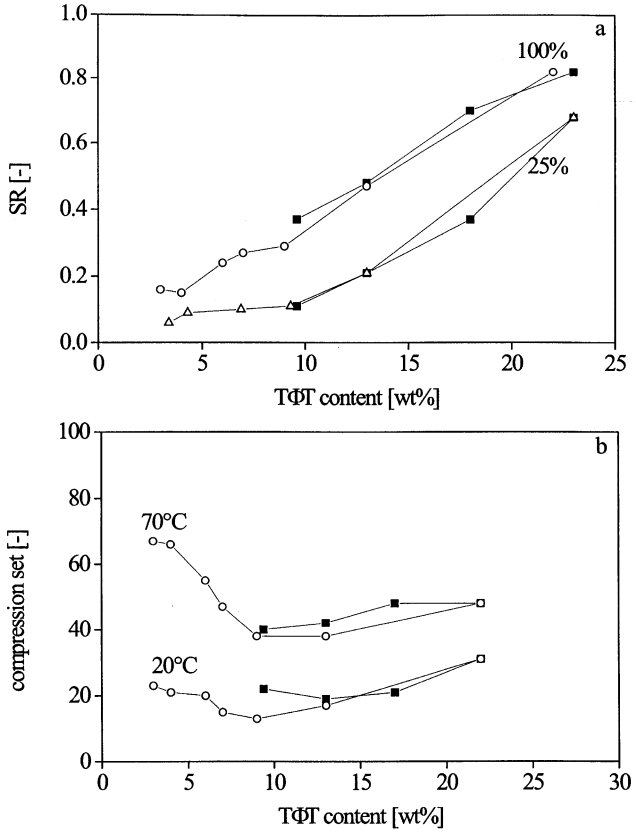

Fig. 12. Influence of TΦT content on elastic properties: (a) stress relaxation at 25 and 100% strain and (b) compression set at room temperature and 70°C (55% compression) versus TΦT content for: (■), TΦT–PTMO; (○), TΦT–$(PTMO_{1000}/DMT)$.

4. Conclusions

The mechanical properties of segmented copolymers with uniform, crystallisable aramid (TΦT) units and PTMO-based soft segments have interesting combination of properties.

The uniform aramid units are very effective in increasing the modulus and the logarithm of the shear modulus at 25°C increases linearly with increasing TΦT content. Another effect of the thin uniform units is that the fracture strains are very high, ranging from 1300 to 2060%. Surprisingly, these fracture strains of the polymers are independent of TΦT content.

The fracture stress increases with the molecular weight of the polymer and the degree of strain-induced crystallisation of the PTMO phase. The effect of the TΦT content on the fracture stress seems to be small. Strain-induced crystallisation gives the polymers a high-fracture stress, however, it leads to a decrease in elasticity. The strain-induced crystallisation can be reduced by lowering of the chain order of PTMO.

The yield stress increases linearly with increasing TΦT content and the yield stress–log modulus relationship is also approximately linear.

A strong strain softening effect was observed. Straining until 160–180% decreased the modulus by a factor of 6–8. The decrease of the modulus is attributed to the disruption of the interconnecting crystalline network. At higher pre-strains, the modulus increases gradually, this probably due to opposing effects: fragmentation of lamellae and orientation of both crystalline and amorphous phases.

Some healing of the modulus is observed with time. This increase in modulus is thought to be due to a reordering of the disrupted crystalline phase.

The elastic behaviour as studied by stress relaxation suggests that the lower the TΦT content the more elastic the material is. However, the compression set results suggest that a too low TΦT concentration is not good either.

Segmented copolyetheresteramides with uniform crystallisable aramid segments and possess a modulus that can be varied over a wide range, the degree of strain-induced crystallisation of the PTMO segments can be adjusted, the fracture strain is extremely high and the low modulus types are highly elastic.

References

[1] Grady BP, Cooper SL. In: Mark JE, Eirich FR, editors. Science and technology of rubber. San Diego: Academic Press, 1978 (chap 13).
[2] Niesten MCEJ, Feijen J, Gaymans RJ. Polymer 2000;41:8487–500.
[3] Niesten MCEJ, Ten Brinke JW, Gaymans RJ. Polymer 2001;42:1461–9.
[4] Woodward AE. Atlas of polymer morphology. Munich: Hanser, 1988 (chap 4).
[5] Young RJ, Lovell PA. Introduction to polymers. 2nd ed. London: Chapman and Hall, 1991 (chap 4, p. 263).
[6] Hiemenz PC. Polymer chemistry, the basic concepts. New York: Marcel Dekker, 1984 (chap 4).
[7] Zhu L, Wegner G. Makromol Chem 1981;182:3625–35.
[8] Sauer BB, McLean RS, Thomas RR. Polym Int 2000;49:449–52.
[9] Wegner G. In: Legge NR, Holden G, Schroeder HE, editors. Thermoplastic elastomers, 1st ed. Munich: Carl Hanser Verlag, 1987 (chap 12).
[10] Young RJ. Mater Forum 1988;11:210–6.
[11] Brooks NW, Unwin AP, Ducket RA, Ward IM. Deformation, yield and fracture of polymers. Churchill Conferences Conference Papers, 1997. p. 52.
[12] Cella RJ. J Polym Sci 1973;Symp No 42:727–40.
[13] Niesten MCEJ, Harkema S, van der Heide E, Gaymans RJ. Polymer 2001;42:1131–42.
[14] Bonart R. J Macromol Sci — Phys 1968;B2(1):115–38.
[15] Ries G, Hurtrez G, Bahadur P. In: Mark, Bikales, Overberger, Menges, editors. Encyclopedia of polymer science and engineering, vol. 2. New York: Wiley, 1989. p. 393–5.
[16] McLean RS, Sauer BB. J Polym Sci: Part B: Polym Phys 1999;37:859–66.
[17] Harrell LL. Macromolecules 1969;2(6):607–12.
[18] Van Hutten PF, Mangnus RM, Gaymans RJ. Polymer 1993;34(20):4193–201.
[19] Miller JA, Shaow BL, Hwang KKS, Wu KS, Gibson PE, Cooper SL. Macromolecules 1985;18(1):32–44.
[20] Dreyfuss P, Dreyfuss MP, Pruckmayr G. In: Mark, Bikales, Overberger, Menges, editors. Encyclopedia of polymer science and engineering, vol. 16. New York: Wiley, 1989. p. 649–76.
[21] McCrum NG, Buckley CP, Bucknall CB. Principles of polymer engineering. Oxford: Oxford University Press, 1988 (chap 1).
[22] Smith P, Matheson RR, Irvine P. Polym Commun 1984;25:294–7.
[23] Brown N. In: Browstow W, Corneliussen RD, editors. Failure of plastics. Munich: Hanser, 1986 (chap 6).
[24] BASF. Lupolen series. Datasheet 1979.
[25] Kubát J, Rigdahl M. In: Browstow W, Corneliussen RD, editors. Failure of plastics. Munich: Hanser, 1986 (chap 4).